International Journal of Rock Mechanics & Mining Sciences 95 (2017) 62–72

Contents lists available at ScienceDirect

International Journal of Rock Mechanics & Mining Sciences

journal homepage: www.elsevier.com/locate/ijrmms

A failure criterion for rocks and concrete based on the Hoek-Brown criterion

Hua Jiang

School of Highway, Chang'an University, Middle Section of South Er Huan Road, Yanta District, Xi'an 710064, China

ARTICLE INFO

Keywords:
Failure criterion
Rocks
Concrete
Triaxial compression
Triaxial extension
Hoek-Brown

ABSTRACT

There have been a number of attempts at developing three-dimensional Hoek-Brown (3D HB) failure criteria with non-circular cross sections to include the effect of the intermediate principal stress for rocks, which is neglected in the classical HB criterion. Those existing 3D HB criteria predict the same strength as the classical HB criterion in triaxial extension (TXE) and triaxial compression (TXC). This paper presents a new failure criterion for rocks and concrete based on a unified expression of the 3D HB failure criteria, which can account for the strength difference between TXE and TXC. The failure cone of the new criterion is convex and smooth everywhere and the deviatoric cross-section of the failure cone can cover various shapes from a curved triangle as the lower bound to a circle as the upper bound. The deviatoric plane locus is controlled by a shape factor k, which can be easily identified from TXE tests. The proposed failure criterion has been validated by biaxial compression tests of concrete, TXC/TXE tests of intact rocks and concrete as well as polyaxial compression (PXC) tests of intact rocks, jointed rock masses and concrete. Results show that the new 3D criterion with an empirical parameter k=−0.99 performs well in characterizing the rock and concrete strength in PXC in the absence of TXE test data. The application of the new criterion to cross-anisotropic rock in PXC is also discussed to show the fabric effect on the rock failure.

1. Introduction

The Hoek-Brown (HB) failure criterion[1] is probably the most popular and widely used nonlinear failure criterion for rock materials with the advantage of less input and easily obtained material parameters. A major limitation of the HB criterion is the independency from the intermediate principal stress σ_2. There have been several modified or three-dimensional (3D) HB failure criteria developed to account for the effect of σ_2, including the studies by Pan and Hudson[2], Priest[3], Zhang and Zhu[4], Benz et al.[5], Melkoumian et al.[6], Jiang et al.[7], Lee et al.[8], Jiang and Zhao[9], Jiang[10].

Among them, Pan and Hudson [2] employed circular sections to describe the deviatoric plane trace, and had uniform meridians between the compressive and tensile meridians of the HB criterion, which abandoned the advantage of the HB criterion in triaxial compression (TXC). The studies by Priest [3] and Melkoumian et al.[6] inherited the compression meridian of the HB criterion, and employed the Druker-Prager (DP) circle in the deviatoric plane, which tended to overestimate the rock strength in many stress conditions like the DP circle circumscribed the Mohr-Coulomb hexagon. The criterion proposed by Zhang and Zhu[4] was neither smooth nor convex in the deviatoric plane, and cannot obtain the failure strength near the singularity zone. The criterion presented by Jiang et al.[7] was smooth but not convex near triaxial extension (TXE) in lower hydrostatic stress. The criterion given by Lee et al.[8] used a smooth and convex Willam-Warnke[11] Lode dependence between compressive and tensile meridians of the HB criterion, and the accuracy depended on the Lode dependence. Benz et al.[5] employed another smooth and convex Lode dependence for their failure criterion, and the formulated criterion was even more complicated than the Lee et al. criterion. Zhang et al.[12] compared three different Lode dependences (Willam-Warnke, Spatial Mobilized Plane, and Yu) to construct the 3D HB criteria and found that no Lode dependence had absolute advantage over others. Jiang and Zhao[9] developed a simple criterion with a similar expression of the HB criterion that can be expressed in terms of the principal stresses. The failure surface was convex everywhere and was smooth except in TXC. More recently, Jiang[10] proposed a 3D failure criterion with smooth and convex failure envelope based on a complicated general Lode dependence, which can incorporate the Willam-Warnke Lode dependence as a special case.

Table 1 summarizes the characteristics of their failure surfaces in the deviatoric and meridian planes. Priest[13] evaluated the performance of several 3D HB failure criteria[2–4] in Table 1 to model the influence of σ_2, and concluded that a substantial amount of further research and

E-mail address: huajiang2006@hotmail.com.

http://dx.doi.org/10.1016/j.ijrmms.2017.04.003
Received 18 July 2016; Received in revised form 30 March 2017; Accepted 15 April 2017
Available online 21 April 2017

Table 1
Summarization of existing 3D HB criteria.

Existing 3D HB criteria	D (θ)	Cross-sectional shape	Cross-sectional characteristic	Meridians inherited from the HB criterion
Pan and Hudson (1988)[2]	1.5	circular	smooth, convex	NA
Priest (2005)[3]	1	circular	smooth, convex	compression
Zhang and Zhu (2007)[4]	$1.5-\cos(\pi/3+\theta)$	non-circular	non-smooth, non-convex	compression and tension
Benz et al. (2008)[5]	NA	non-circular	smooth, convex	compression and tension
Melkoumian et al. (2009)[6]	1	circular	smooth, convex	compression
Jiang et al. (2011)[7]	$1.5-0.5\cos 3\theta$	non-circular	smooth, non-convex	compression and tension
Lee et al. (2012)[8]	NA	non-circular	smooth, convex	compression and tension
Jiang and Zhao (2015)[9]	$2\cos(\pi/3-\theta)$	non-circular	non-smooth, convex	compression and tension
Jiang (2017)[10]	NA	non-circular	smooth, convex	compression and tension

Note: NA-Not applicable.

rock testing should be conducted before any of them can be applied with confidence. Besides, existing 3D HB criteria with non-circular cross sections[4–9] predict the same strength in TXC ($\sigma_2=\sigma_3<\sigma_1$) and TXE ($\sigma_2=\sigma_1>\sigma_3$) for rocks as the HB criterion does because both the compression and extension meridians of the HB criterion are inherited. Hence, the negligence of the effect of σ_2 still exists in TXE in those failure criteria by comparing the strength in TXE and that in TXC for a given σ_3.

In comparison, much of the conventional triaxial test for rocks confirmed that the stresses required to fail the rock in TXE are generally higher by 10–20% than those obtained from TXC.[14–17] Similar findings are reported for concrete materials.[18,19] It is also reported[20,21] that the equibiaxial compression strength of concrete $f_{cc}^{'}$ is around 1.15–1.16 times of uniaxial compression strength of concrete σ_{ci} , which means that the concrete strength in TXE is 15–16% higher than that in TXC when σ_3 =0.

There is indeed a practical need to develop a new 3D failure criterion, which can take into account of the characteristic that the strength in TXE is higher than that in TXC for both rock and concrete materials. In this study, a new failure criterion based on a unified expression of the 3D HB criteria is proposed to meet the practical needs. The failure surface of the new criterion is bounded by the failure surfaces of two existing 3D HB criteria, and is convex and smooth everywhere, which is convenient for numerical modeling. Moreover, the application of the proposed failure criterion is expanded to concrete materials under varies stress states. Finally, by incorporating the fabric effect on the failure strength, an extension of the new criterion to cross-anisotropic rock in PXC is discussed.

2. Preliminaries

The failure function for a strength criterion is usually expressed in terms of the principal stresses $f(\sigma_1, \sigma_2, \sigma_3)$, or the stress invariants $f(I_1, J_2, \theta)$, $f(\xi, \rho, \theta)$. Fig. 1 shows the Haigh–Westergaard coordinates (ξ, ρ, θ) for geometry interpretation, where ξ is the projection on the unit vector $\bar{e}=(1, 1, 1)/\sqrt{3}$ on the hydrostatic axis, the radial distance from the failure point P to the hydrostatic axis N is given by ρ, and the similarity angle $\theta(0\le\theta\le\pi/3)$ is the measure of a rotation from axis S_1.

$$\xi=|\overrightarrow{\mathrm{ON}}|=I_1/\sqrt{3} \tag{1}$$

$$\rho=|\overrightarrow{\mathrm{NP}}|=\sqrt{2J_2} \tag{2}$$

$$\theta=\frac{1}{3}\arccos\left(\frac{3\sqrt{3}}{2}\frac{J_3}{\sqrt{J_2^3}}\right) \tag{3}$$

where $I_1=\sigma_{ii}$ is the first invariant of the stress tensor σ_{ij}, while $J_2=S_{ij}S_{ji}/2$ and $J_3=S_{ij}S_{jk}S_{ki}/3$ are the second and third invariants of the deviatoric stress tensor $S_{ij}=\sigma_{ij}-\sigma_{kk}\delta_{ij}/3$. The principal stresses can be expressed in terms of the stress invariants as [9,10].

$$\sigma_1=\frac{I_1}{3}+\frac{2}{\sqrt{3}}\sqrt{J_2}\cos\theta \tag{4}$$

$$\sigma_2=\frac{I_1}{3}+\frac{2}{\sqrt{3}}\sqrt{J_2}\cos\left(\frac{2\pi}{3}-\theta\right) \tag{5}$$

$$\sigma_3=\frac{I_1}{3}+\frac{2}{\sqrt{3}}\sqrt{J_2}\cos\left(\frac{2\pi}{3}+\theta\right) \tag{6}$$

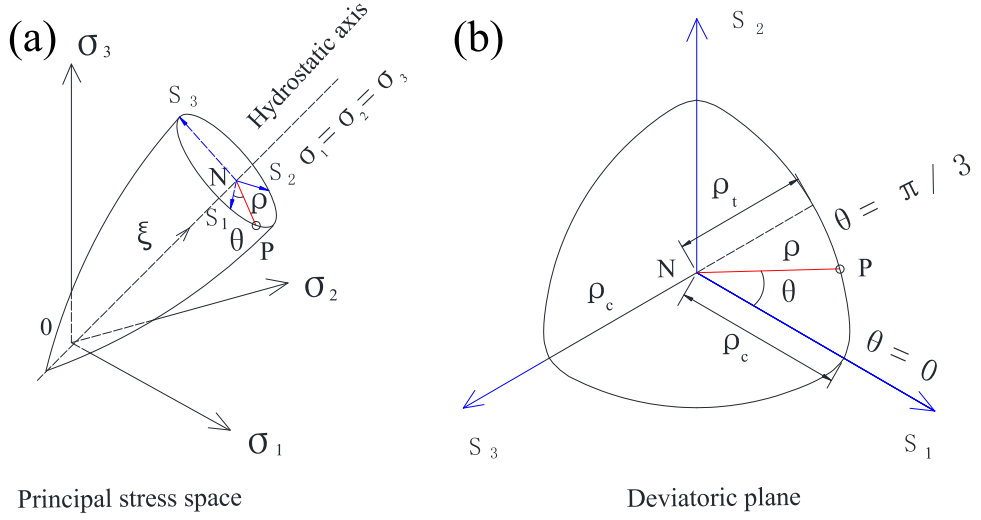

Fig. 1. Haigh–Westergaard space and Principal stress space.

3. A unified expression of the three-dimensional Hoek–Brown failure criteria for rocks

The HB failure criterion is an empirical criterion developed from the curve-fitting TXC test data. The failure function assumes that the rock failure is controlled by the major and minor effective principal stresses (with primes), σ_1' and σ_3'

$$\sigma_1' - \sigma_3' = \sigma_{ci}\left(m_b\frac{\sigma_3'}{\sigma_{ci}} + s\right)^a \tag{7}$$

where the intermediate effective principal stress σ_2' is not considered in above expression, and the compression stresses are taken positive throughout this paper; σ_{ci} is the uniaxial compression strength of the intact rock with petrographic constant m_i (analogous to the frictional strength of the rock); the dimensionless empirical constants m_b is a reduced value of m_i to account for the strength reducing effects of the rock mass; s ($0\le s\le 1$) (a measure of rock cohesion) and a for broken rocks can be estimated from the geological strength index GSI and the disturbance of rock masses D ($0\le D\le 1$) due to near surface blast damage and stress relaxation.[1,22]

$$m_b = m_i\exp\left(\frac{GSI-100}{28-14D}\right) \tag{8}$$

$$s = \exp\left(\frac{GSI-100}{9-3D}\right) \tag{9}$$

$$a = \frac{1}{2} + \frac{1}{6}\left[\exp\left(\frac{-GSI}{15}\right) - \exp\left(\frac{-20}{3}\right)\right] \tag{10}$$

According to Eq. (7), the rock strength only depends on σ_3' regardless a variation of the stress state from $\sigma_2' = \sigma_3'$ corresponding to TXC to $\sigma_2' = \sigma_1'$ corresponding to TXE.

Substituting Eqs. (4) and (6) into Eq. (7), then the HB criterion can be expressed in terms of the stress invariants as

$$\left[B(\theta)\frac{\sqrt{J_2'}}{\sigma_{ci}}\right]^{1/a} + C(\theta)\frac{m_b}{3}\frac{\sqrt{3J_2'}}{\sigma_{ci}} - \frac{m_b}{3}\frac{I_1'}{\sigma_{ci}} = s \tag{11}$$

with

$$B(\theta) = 2\sin(\pi/3+\theta) \text{and} C(\theta) = 2\cos(\pi/3-\theta) \tag{12}$$

Fig. 2 plots $B(\theta)$ and $C(\theta)$ versus θ as θ varies from 0 to π/3. It can be observed that $B(\theta)$ is symmetry with respect to θ=π/6(see the vertical dash line in the middle of the figure), and has $B(0) = B(\pi/3) = \sqrt{3}$ at two ends, whereas $C(\theta)$ is a monotonically increasing function from 1 to 2.

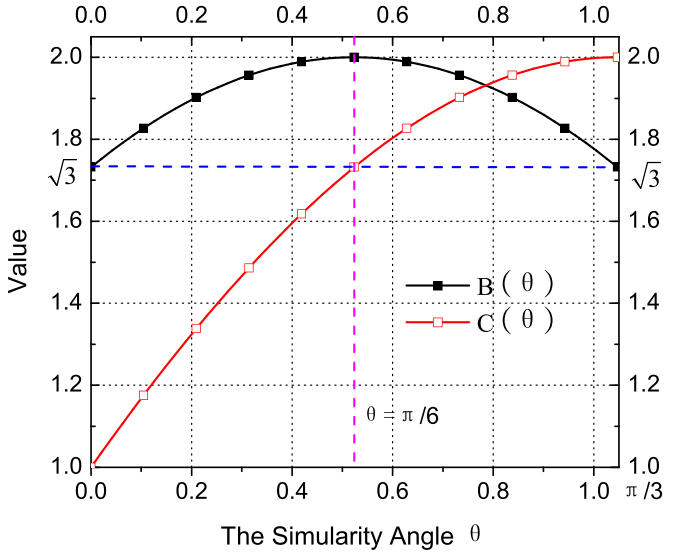

Fig. 2. Plot of B(θ) and C(θ) as functions of θ.

Setting $B(\theta) = \sqrt{3}$ (see the horizontal dash line in Fig. 2) and replacing $C(\theta)$ by a new function $D(\theta)$, then Eq. (11) takes the form

$$\left(\frac{\sqrt{3J_2'}}{\sigma_{ci}}\right)^{1/a} + D(\theta)\frac{m_b}{3}\frac{\sqrt{3J_2'}}{\sigma_{ci}} - \frac{m_b}{3}\frac{I_1'}{\sigma_{ci}} = s \tag{13}$$

which refers to a unified expression of most of existing 3D HB criteria,[9] and the term $D(\theta)$ varies, depending on the criterion adopted (see Table 1). All existing 3D HB criteria summarized in Table 1 have the same number of material parameters as the HB criterion, among which only the Jiang-Zhao 3D HB criterion has a similar simple expression as that of the HB criterion in terms of the principal stresses.[9] The failure criteria with non-circular cross sections give the same strength in TXC and TXE because both compression and extension meridians of the HB criterion are inherited in their failure surfaces.

4. A new failure criterion for rocks and concrete based on the Hoek-Brown criterion

4.1. Failure function of the new criterion

To construct a new 3D failure criterion which can account for the strength difference between TXE and TXC states, a possible expression can be derived based on the unified expression shown in Eq. (13).

$$\left(\frac{\sqrt{3J_2'}}{\sigma_{ci}}\right)^{1/a} + A(k,\theta)\frac{m_b}{3}\frac{\sqrt{3J_2'}}{\sigma_{ci}} - \frac{m_b}{3}\frac{I_1'}{\sigma_{ci}} = s \tag{14}$$

with

$$A(k,\theta) = \cos\left[\frac{1}{3}\arccos(k\cos 3\theta)\right] / \cos\left[\frac{1}{3}\arccos(k)\right] \tag{15}$$

where k ($-1\le k\le 0$) is a shape factor, which governs the deviatoric plane shape of the new failure criterion (see Fig. 4). Material parameters such as m_b, σ_{ci} and k involved in the new failure criterion will be calibrated in Section 4.2.

Differentiating $A(k,\theta)$ with respect to θ, results in

$$\frac{dA(k,\theta)}{d\theta} = \frac{k\sin 3\theta}{\sqrt{1-k^2\cos^2 3\theta}}\frac{\sin[\frac{1}{3}\arccos(k\cos 3\theta)]}{\cos[\frac{1}{3}\arccos(k)]} \tag{16}$$

Then $\frac{dA(k,\theta)}{d\theta}_{\theta=0,k\neq -1} = \frac{dA(k,\theta)}{d\theta}_{\theta=\pi/3} = 0$ can be obtained from Eq. (16). Fig. 3 shows $A(k,\theta)$ as functions of θ for five different k: $A(k,\theta)$ is a monotonically increasing function for each k with an initial value 1 at θ=0, and tends to decrease with an increase of k; those curves have two zero slope ends when $k\neq -1$, which can be verified from Eq. (16); the curve corresponding to k=−1 appears the same shape as the curve of $C(\theta)$ shown in Fig. 2, which can be confirmed mathematically by comparing Eq. (12) with Eq. (18). When k=0,

$$A(k,\theta) = A(0,\theta) = 1 \tag{17}$$

and Eq. (14) becomes the compressive meridian of the HB criterion or the failure function of the Priest 3D HB criterion (see Table 1). When k=−1,

$$A(k,\theta) = A(-1,\theta) = 2\cos\left[\frac{1}{3}\arccos(-\cos 3\theta)\right] = 2\cos(\pi/3-\theta) = C(\theta) \tag{18}$$

and Eq. (14) reduces to the failure function of the Jiang-Zhao 3D HB criterion listed in Table 1:

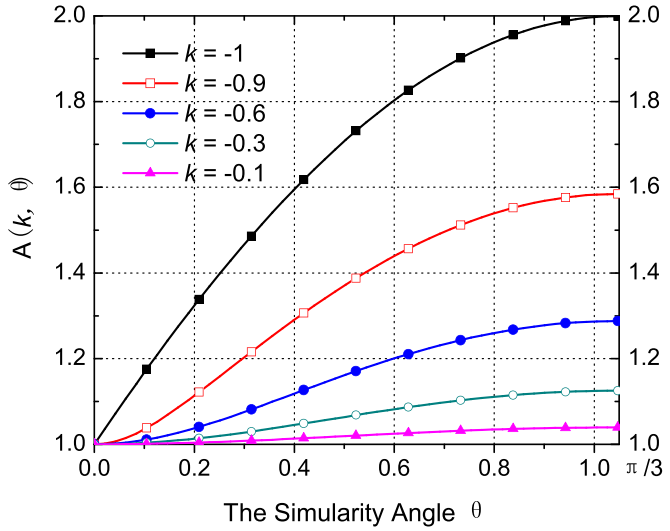

Fig. 3. Plot of $A(k, \theta)$ as functions of θ at various value of k.

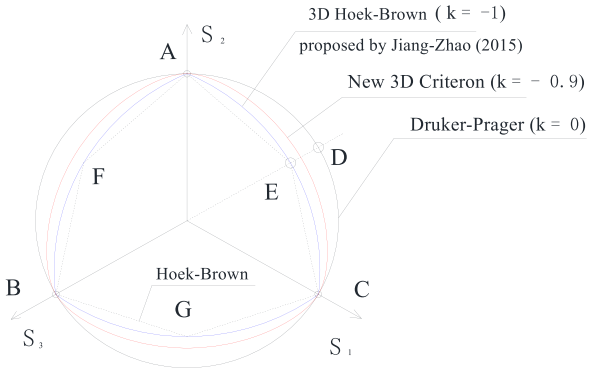

Fig. 4. Representation of effect of k on failure locus of the new failure criterion on the deviatoric plane when m_i =10, s=1, and a =0.5.

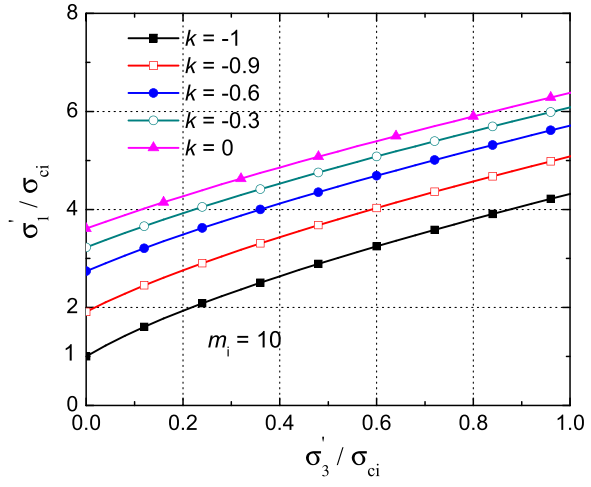

Fig. 5. Relationship between σ_1' and σ_3' at various value of k in TXE.

$$\left(\frac{\sqrt{3J_2'}}{\sigma_{ci}}\right)^{1/a} + 2\cos(\pi/3-\theta)\frac{m_b}{3}\frac{\sqrt{3J_2'}}{\sigma_{ci}} - \frac{m_b}{3}\frac{I_1'}{\sigma_{ci}} = s \tag{19}$$

Fig. 4 shows the influence of k on failure locus of the proposed 3D criterion in the deviatoric plane with m_i =10, s=1, a =0.5 and I_1'/σ_{ci} = 4 for illustration purposes. The locus is a circle of the Drucker-Prager (DP) criterion when k=0, and is a curved triangle of the Jiang-Zhao 3D HB criterion that circumscribes the HB locus (represented by the dash line) when k=−1. The locus corresponding to other k ($-1 < k < 0$) lies inside the DP circle and outside the Jiang-Zhao curved triangle. We know that the DP circle always over-predicts the rock strength especially near TXE state (see point D), and the Jiang-Zhao curved triangle may underestimate the strength near TXE state (see point E) as pointed out in the introduction section. Hence, developing a new 3D criterion with its deviatoric plane locus within two bounds is reasonable.

It is also worth noted that the failure envelope surface corresponding to k ($-1 < k \le 0$) is convex and smooth everywhere, and coincides with that of the HB criterion only in TXC state. The failure envelope surface of the Jiang-Zhao 3D HB criterion is convex everywhere but not smooth when θ=0 (see Points A, B and C). When θ = 0:

$$A(k, \theta) = A(k, 0) = 1 \tag{20}$$

When $\theta = \pi/3$:

$$A(k, \theta) = A(k, \pi/3) = \cos\left[\frac{1}{3}\arccos(-k)\right] / \cos\left[\frac{1}{3}\arccos(k)\right] \tag{21}$$

According to Eqs. (14) and (21), the extension meridian of the new criterion can be represented by

$$\left(\frac{\sqrt{3J_2'}}{\sigma_{ci}}\right)^{1/a} + \frac{m_b}{3}\frac{\cos\left[\frac{1}{3}\arccos(-k)\right]}{\cos\left[\frac{1}{3}\arccos(k)\right]}\frac{\sqrt{3J_2'}}{\sigma_{ci}} - \frac{m_b}{3}\frac{I_1'}{\sigma_{ci}} = s \tag{22}$$

For intact rocks (GSI=100), a=0.5, $m_b = m_i$ and s=1 are obtained from Eqs. (8), (9) and (10), then the failure function of the proposed failure criterion given by Eq. (14) is reduced to

$$\frac{3J_2'}{\sigma_{ci}^2} + \frac{m_i}{3}\frac{\cos\left[\frac{1}{3}\arccos(k\cos 3\theta)\right]}{\cos\left[\frac{1}{3}\arccos(k)\right]}\frac{\sqrt{3J_2'}}{\sigma_{ci}} - \frac{m_i}{3}\frac{I_1'}{\sigma_{ci}} = 1 \tag{23}$$

Substituting θ=0 into Eq. (23), the compressive meridian ($\sigma_2' = \sigma_3' < \sigma_1'$) takes the form of

$$\frac{3J_2'}{\sigma_{ci}^2} + \frac{m_i}{3}\frac{\sqrt{3J_2'}}{\sigma_{ci}} - \frac{m_i}{3}\frac{I_1'}{\sigma_{ci}} = 1 \tag{24}$$

Substituting θ=π/3 into Eq. (23), the tensile meridian ($\sigma_2' = \sigma_1' > \sigma_3'$) is given by

$$\frac{3J_2'}{\sigma_{ci}^2} + \frac{m_i}{3}\frac{\cos\left[\frac{1}{3}\arccos(-k)\right]}{\cos\left[\frac{1}{3}\arccos(k)\right]}\frac{\sqrt{3J_2'}}{\sigma_{ci}} - \frac{m_i}{3}\frac{I_1'}{\sigma_{ci}} = 1 \tag{25}$$

which can be also obtained by substituting a=0.5 into Eq. (22). Eq. (25) can be further expressed in terms of the principal stresses

$$\frac{(\sigma_1' - \sigma_3')^2}{\sigma_{ci}^2} + \frac{m_i}{3}\frac{\cos\left[\frac{1}{3}\arccos(-k)\right]}{\cos\left[\frac{1}{3}\arccos(k)\right]}\frac{\sigma_1' - \sigma_3'}{\sigma_{ci}} - \frac{m_i}{3}\frac{2\sigma_1' + \sigma_3'}{\sigma_{ci}} = 1 \tag{26}$$

When k=−1, Eq. (26) becomes Eq. (7) with a=0.5, and s=1, which denotes for the tension meridian of the HB criterion in terms of the principal stresses.

A non-linear relationship between σ'_1 and σ'_3 calculated with Eq. (26) is shown in Fig. 5. The lower bound of those curves corresponds to k=−1, and the upper bound of those curves corresponds to k=0.

4.2. Calibration of the new failure criterion

For intact rocks and concrete, there are usually three unknown parameters m_i, σ_{ci} and k involved in Eq. (23), which can be determined using following approaches corresponding to different stress states. In some cases, σ_{ci} is known from the tests and only two parameters left in Eq. (23).

In conventional triaxial test, m_i and σ_{ci} can be determined from TXC using the best fitting method according to the compression meridian

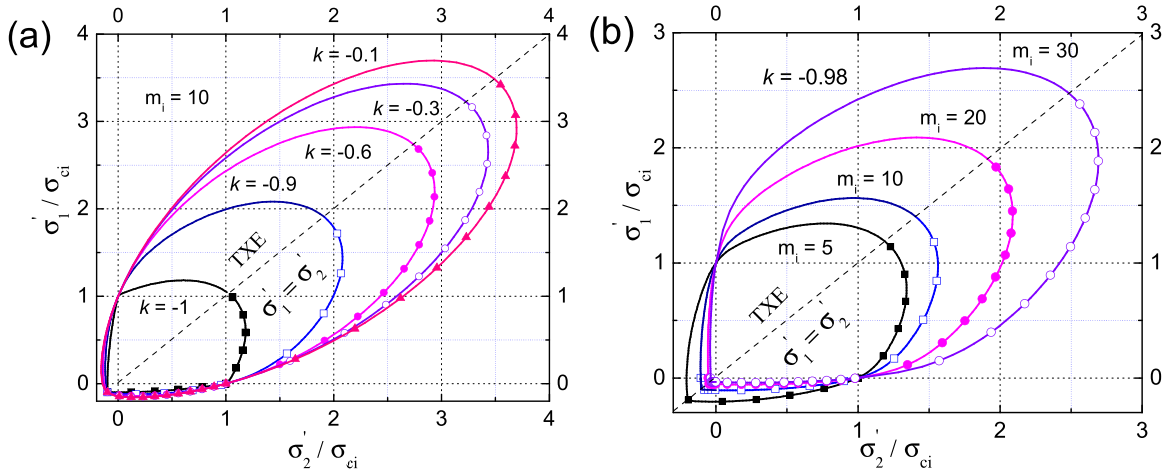

Fig. 6. The new failure criterion in biaxial principal stress plane: (a) at various value of k with m_i=10, (b) at various value of m_i with k=−0.98.

Table 2
Test data source and prediction results using the new failure criterion for rocks and concrete.

	Rock/Concrete type	Test data source	σ_{ci}	m_i	k	DC (TXC /TXE)
1	Concrete-TXC /TXE	Mills and Zimmerman (1970)[18]	23.30	12.29	−0.9778	0.9874/0.9671
2	Phra Wihan sandstone-TXC /TXE	Phueakphum et al. (2013)[17]	NA	17.07	−0.9946	0.9892/0.9514
3	Phu Kradung siltstone- TXC /TXE	Phueakphum et al. (2013)[17]	NA	16.45	−0.9846	0.9711/0.9786
4	Phu Phan sandstone- TXC /TXE	Phueakphum et al. (2013)[17]	NA	9.46	−0.9602	0.9785/0.9377
5	Saraburi marble-TXC /TXE	Phueakphum et al. (2013)[17]	NA	16.86	−0.9889	0.9503/0.9613
6	Concrete-Biaxial compression	Kupfer et al. (1969) [20]	NA	11.32	−0.9975	NA
7	Concrete-PXC	Mills and Zimmerman (1970)[18]	23.30	12.29	−0.9778	0.9874/0.9671
8	Manazuru andesite- PXC	Mogi (2007)[16]	(140)	34.2	−0.99	0.997/ NA
9	Mizuho trachyte- PXC	Mogi (2007)[16]	(100)	11.1	−0.99	0.990/ NA
10	Solnhofen limestone- PXC	Mogi (2007)[16]	(310)	4.6	−0.99	0.959/ NA
11	KTB amphibolite- PXC	Colmenares and Zoback (2002)[23]	195.9	29.4	−0.99	0.997/ NA
12	Yuubari shale- PXC	Colmenares and Zoback (2002)[23]	57.2	11.2	−0.99	0.976/ NA
13	Jointed biotite granite-PXC	Müller-Salzburg and Ge (1983)[24]	NA	NA	NA	NA
14	Anisotropic rock-UC	Pietruszczak et al. (2002)[27]	NA	NA	NA	NA

Note: NA-Not applicable, UC-uniaxial compression, () refers to the UC data obtained from the tests.

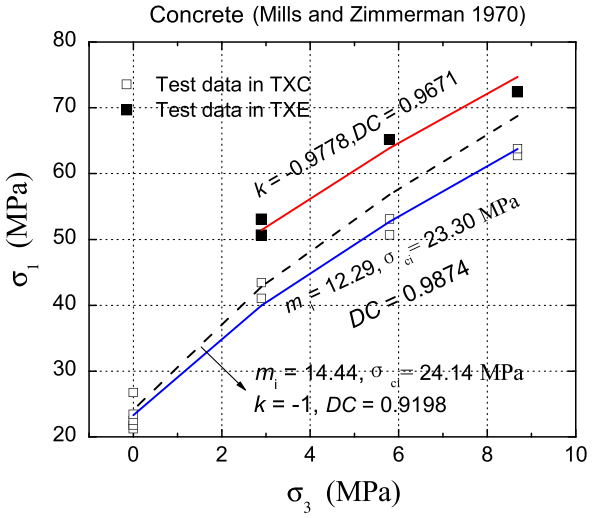

Fig. 7. Comparison between the predicted failure strength and the test data in triaxial compression/extension for Concrete. The dash line represents the Jiang-Zhao failure criterion.

given by Eq. (24), and then the fitting of parameter k can be performed from TXE according to the tension meridian shown in Eq. (25) with fixed m_i and σ_{ci} obtained from Eq. (24).

In polyaxial compression (PXC) test, m_i, σ_{ci} and k are fitted from TXC and TXE as introduced above. After that, these parameters are used to predict the failure strength in other loading conditions because determination of material parameters using PXC data is expensive and such testing facilities are not generally available.

In biaxial plane-stress condition, the process of determining material parameters and the influence of the intermediate principal stress on the failure strength are shown as follows.

4.2.1. Parameter determination in biaxial plane-stress condition

In biaxial plane-stress condition, the parameter k in Eq. (26) can be obtained using the uniaxial tension strength ($\sigma'_1 = \sigma'_2 = 0$, $\sigma'_3 = -f'_t < 0$) and equibiaxial compression strength ($\sigma'_1 = \sigma'_2 = f'_{cc} > 0$, $\sigma'_3 = 0$) because two stress states lie in the tensile meridian of the new failure criterion. Substituting two stress states into Eq. (26), one can obtain

$$\frac{\cos[\frac{1}{3}\arccos(k)]}{\cos[\frac{1}{3}\arccos(-k)]} = \frac{m_i}{3/(f'_t/\sigma_{ci}) - 3f'_t/\sigma_{ci} - m_i} \tag{27}$$

and

$$\frac{\cos[\frac{1}{3}\arccos(k)]}{\cos[\frac{1}{3}\arccos(-k)]} = \frac{m_i}{3/(f'_{cc}/\sigma_{ci}) + 2m_i - 3f'_{cc}/\sigma_{ci}} \tag{28}$$

Then the parameter m_i can be obtained by combining Eq. (27) with Eq. (28):

$$m_i = 1/(f'_t/\sigma_{ci}) - 1/(f'_{cc}/\sigma_{ci}) - f'_t/\sigma_{ci} + f'_{cc}/\sigma_{ci} \tag{29}$$

For concrete material, $1.15 \le f'_{cc}/\sigma_{ci} \le 1.20$ and $0.05 \le f'_t/\sigma_{ci} \le 0.1$ are reported by Kupfer [17], then the estimated m_i according to Eq. (29) is in the range 10.18–20.32, and the estimated k according to Eq. (27)

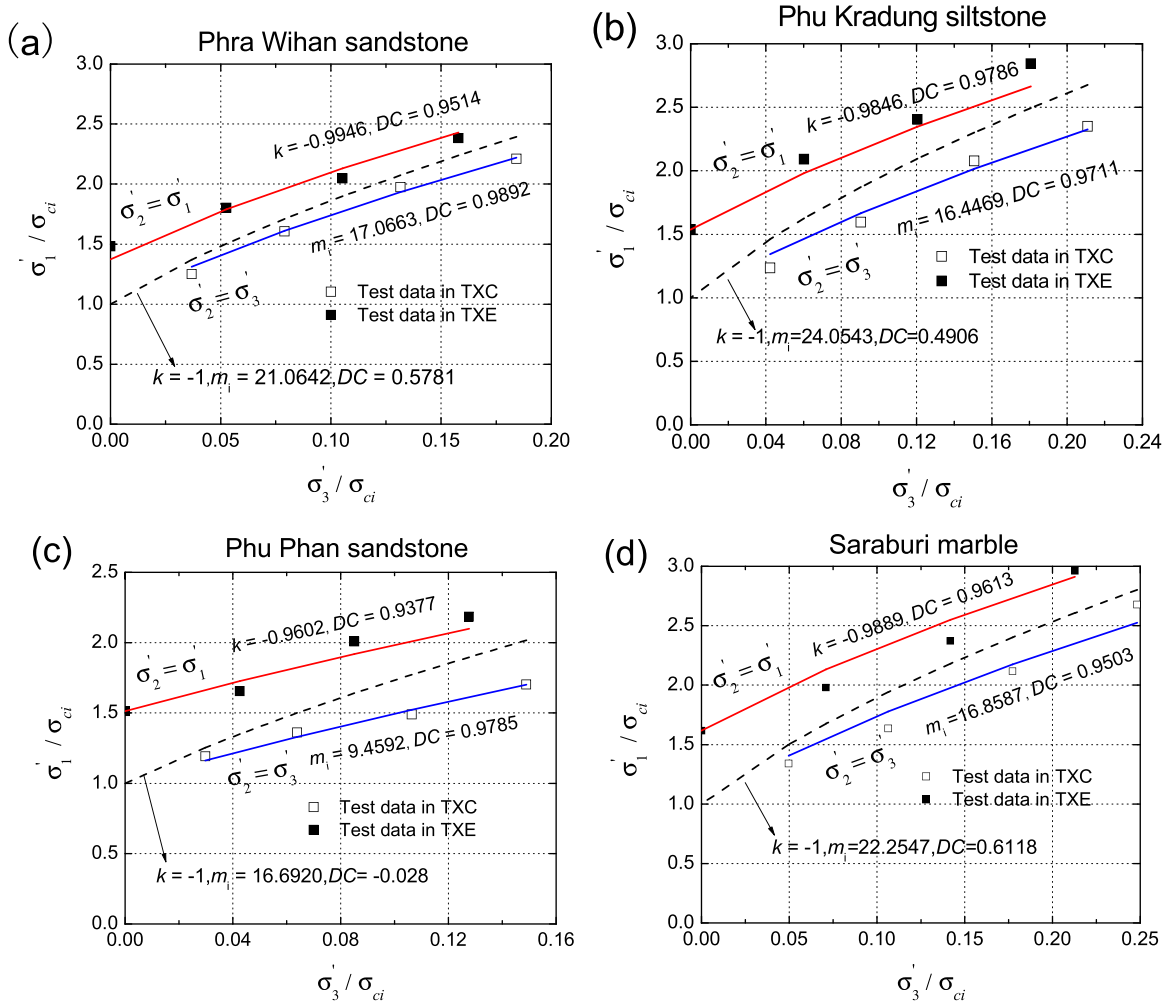

Fig. 8. Comparison between the predicted failure strength and the test data in triaxial compression/extension for rocks. The dash line represents the Jiang-Zhao 3D HB criterion.

varies from −0.9993 to −0.9972.

If f'_{cc} is unavailable, and we have equibiaxial tension ($\sigma'_1 = 0$, $\sigma'_2 = \sigma'_3 = -f'_{tt} < 0$) in hand, then m_i can be derived by substituting the equibiaxial tension state into the compression meridian of the new failure criterion in Eq. (24), the result is

$$m_i = 1/(f'_{tt}/\sigma_{ci}) - f'_{tt}/\sigma_{ci} \tag{30}$$

If taking $f'_{tt} = f'_t$, then m_i can be estimated as $1/(f'_t/\sigma_{ci}) - f'_t/\sigma_{ci}$. When $0.05 \le f'_t/\sigma_{ci} \le 0.1$ is used for concrete, m_i is in the range 9.9–19.95, which is close to the estimated value 10.18–20.32) from Eq. (29). When m_i is known, the parameter k can be obtained from Eq. (27).

4.2.2. The new failure criterion in biaxial plane-stress condition

The effect of the intermediate principal stress can be clearly shown in $\sigma'_1 - \sigma'_2$ space for a given σ'_3. When $\sigma'_3 = 0$, $\sigma'_1 - \sigma'_2$ plane is called biaxial plane (plane stress). In Figs. 6a and b, the dash lines represent TXE state with $\sigma'_1 = \sigma'_2$, and the intersection of the failure envelope and dash line is f'_{cc}. Because the stress state of equibiaxial compression can be regarded a special case of TXE ($\sigma'_2 = \sigma'_1 = f'_{cc} > \sigma'_3 = 0$) and uniaxial compression can be viewed as a special case of TXC ($\sigma'_1 = \sigma_{ci} > \sigma'_2 = \sigma'_3 = 0$), then f'_{cc}/σ_{ci} is a stress ratio of TXE to TXC when $\sigma'_3 = 0$, which can directly show the strength variation from TXE to TXC.

Fig. 6a shows the failure surface envelope at different $k(-1 \le k \le -0.1)$ when m_i =10 in biaxial plane-stress state ($\sigma'_3 = 0$). It is noted that f'_{cc} equals to σ_{ci} only when k=−1, and biaxial compression strength in other stress combinations is larger than σ_{ci}. σ'_1/σ_{ci} increases monotonically with k and σ'_2/σ_{ci}. In comparison, the influence of k on the biaxial tension and tension-compression strength is negligible. The equibiaxial tension strength f'_{tt} is a constant for a given m_i, which can be determined from Eq. (30).

Fig. 6b demonstrates the biaxial compression strength for different value of $m_i(5 \le m_i \le 30)$ when k=−0.98. The biaxial compression strength increases significantly as an increase of m_i, the biaxial tension and tension-compression strength are also influenced by m_i.

5. Validation of the new failure criterion for rocks and concrete

To validate the new failure criterion, biaxial compression, TXC/TXE and PXC tests for intact rocks and concrete, PXC tests for rock masses as well as uniaxial compression tests for cross-anisotropic rock have been used in this section. Table 2 summarizes the open literatures where the experimental data of rocks and concrete was taken.

5.1. Conventional triaxial test of concrete and rocks

Fig. 7 shows a comparison of the model prediction with the experimental data of conventional triaxial tests for concrete reported by Mills and Zimmerman [18]. The fitting m_i and σ_{ci} in TXC is 12.2471 and 23.30 MPa, respectively. The fitting parameter k in TXE is −0.9778. It can be seen that the predicted failure stress in TXE (see the top solid or the red line) is notably higher than that in TXC (see the bottom solid or the blue line), which agrees excellent well with the test data. In comparison, the fitting result using the Jiang-Zhao 3D HB criterion

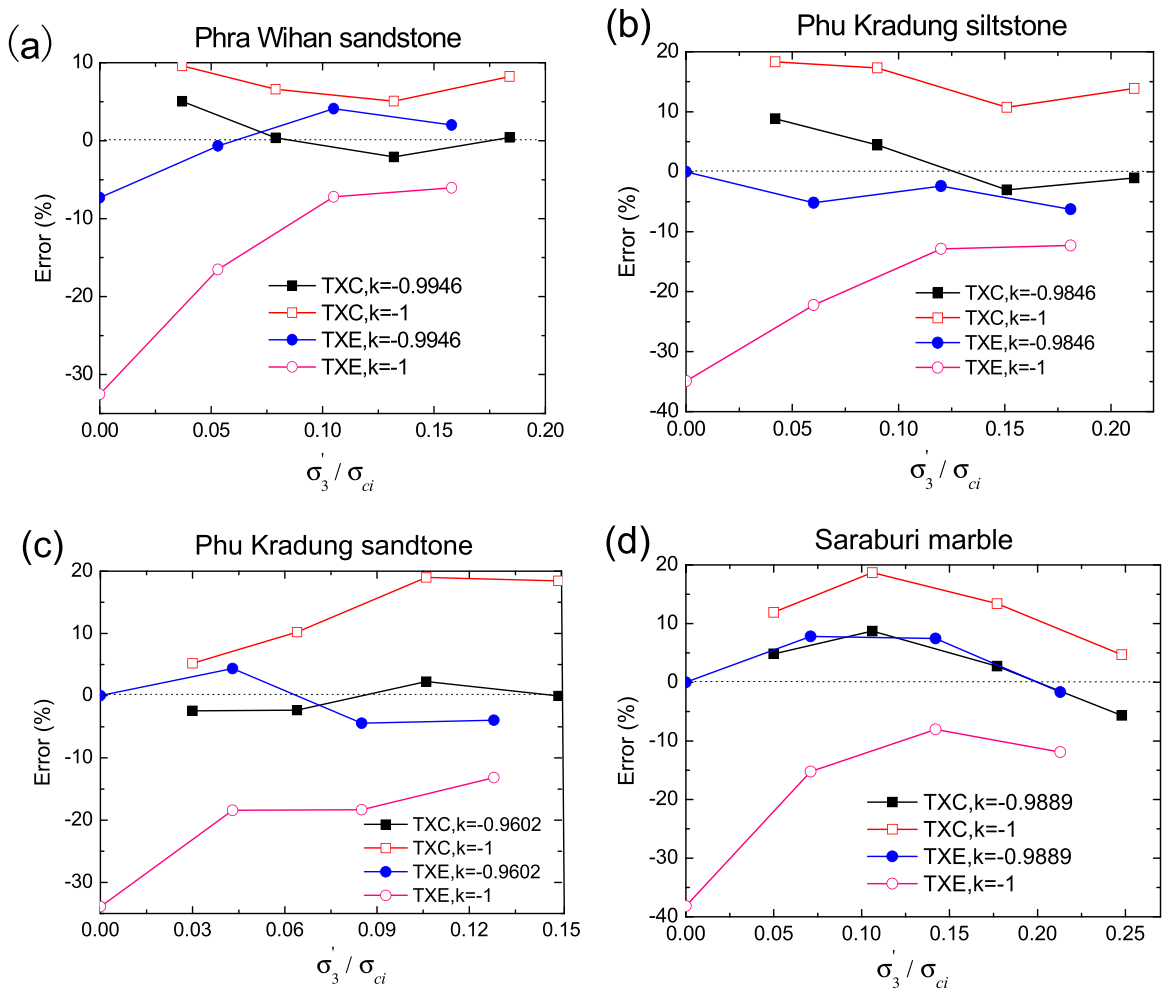

Fig. 9. Comparison of the prediction error for concrete and rocks using the new criterion and Jiang-Zhao 3D HB criterion.

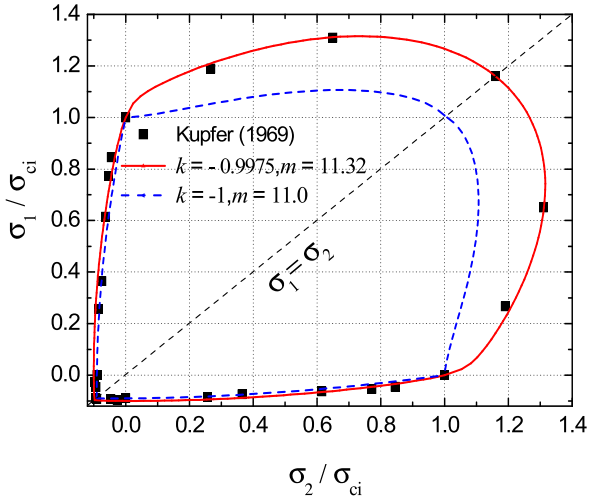

Fig. 10. Comparison between the predicted failure envelope and the biaxial compression data for concrete using the new criterion and Jiang-Zhao 3D HB criterion.

corresponding to k=−1 is illustrated in a single dash line in the same figure, and the fitting m_i and σ_{ci} is 14.14 and 24.14 MPa, respectively. Obviously, two separated fitting curves obtained using the new failure criterion is superior to a single fitting curve obtained using the Jiang-Zhao 3D HB criterion, which can be also seen from the coefficient of determination (*DC*).It's important to note that σ_{ci} is also fitted numerically because there is large discreteness for σ_{ci} in the test data.

Figs. 8a-d compare the predicted curve using the new failure criterion with the test data in TXC and TXE for four different rock types. The test data is normalized by σ_{ci} because σ_{ci} is known from the tests. The agreement between the experimental data and theoretical prediction is very good for all rock types, which confirms that the strength in TXE higher than the strength in TXC can be well captured by the new failure criterion. The fitting k in TXE is in the range −0.9602 to −0.9946, and the corresponding *DC* is in the range 0.9377–0.9786 (also see Table 2). In comparison, the Jiang-Zhao failure criterion underestimates the rock strength in TXE and overestimates the strength in TXC for all four rocks. The best-fitting *DC* is in the range −0.028 to 0.6118, which is much lower than *DC* obtained from two separated fitting curves for TXE and TXC, respectively. It is worth noting that a negative *DC* (−0.028) is obtained for Phu Phan sandstone, which means that the chosen model (the Jiang-Zhao 3D HB criterion) does not follow the trend of the data, and the fitting line is worse than a horizontal line.

The prediction error for rocks is plot in Figs. 9a-d, where error ε is defined as $100(\sigma_1'_{theoritical} - \sigma_1'_{test})/\sigma_1'_{test}$. $|\varepsilon|$ obtained from the new failure criterion is much smaller than that resulted from the Jiang-Zhao failure criterion with k=−1 except for one TXC case for Saraburi marble. The overestimation the strength in TXC and the underestimation the strength in TXE resulted from the Jiang-Zhao criterion can be further confirmed.

5.2. *Biaxial compression and polyaxial compression tests of concrete and rocks*

Fig. 10 compares the biaxial failure envelope of the proposed 3D

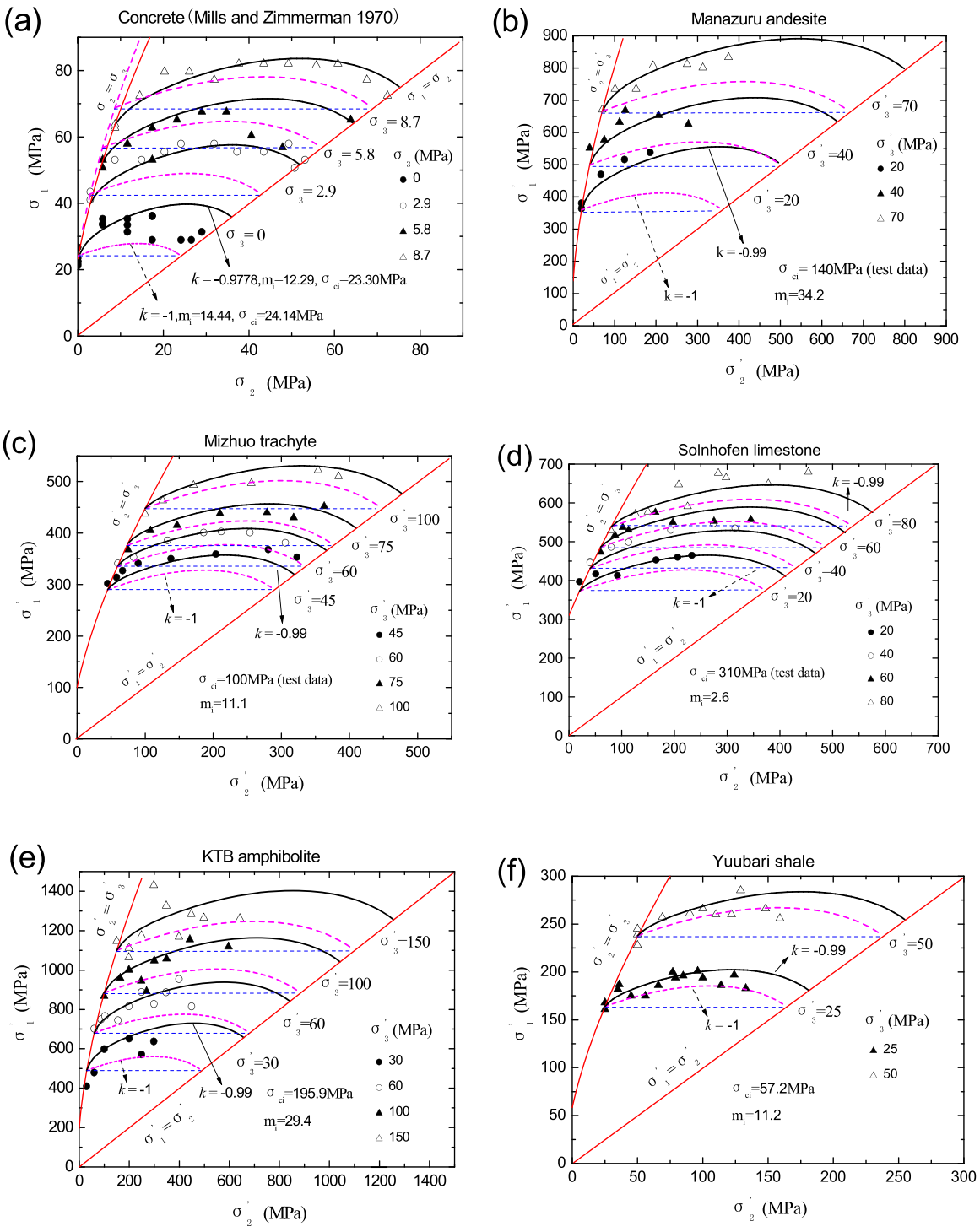

Fig. 11. Comparison of the best-fit failure envelope with polyaxial compression test data of concrete and rocks. The curved dash line represents the Jiang-Zhao 3D HB criterion.

failure criterion with the test data for concrete reported by Kupfer.[20] The material parameter $m_i = 11.32$ is obtained by substituting the test data $f_t'/\sigma_{ci} = 0.09$ and $f_{cc}'/\sigma_{ci} = 1.16$ into Eq. (29), and the shape factor k is further obtained by substituting $m_i = 11.32$ and $f_{cc}'/\sigma_{ci} = 1.16$ into Eq. (28). Clearly the theoretical curve corresponding to $k = -0.9975$ and $m_i = 11.32$ agrees sufficiently well with the test data. The dash line represents the predicted results using the Jiang-Zhao failure criterion with $k = -1$, $m_i = 11.0$, which tends to underestimate the failure strength in compression region.

Fig. 11a compares the predicted strength with the test data for concrete in the $\sigma'_1 - \sigma'_2$ plane grouped by σ'_3. In those figures, the symbols refer to the actual PXC test data, and test data with the same σ'_3 is indicated by the same symbol; solid lines represent the predicted relationship for σ'_1 and σ'_2 corresponding to the best-fitting parameters obtained from conventional triaxial test (see Fig. 7). It is clearly shown that the prediction fits the test data quite well for concrete especially at high σ'_3. In comparison, the prediction curve using the Jiang-Zhao failure criterion corresponding to k=−1 is also plotted (see dash line), which tends to underestimate the measured strength.

Figs. 11b to 11f show the comparisons of the model prediction and various reported data of five rocks. In the numerical curves, k is empirically set to be −0.99 because no TXE tests of rocks were reported

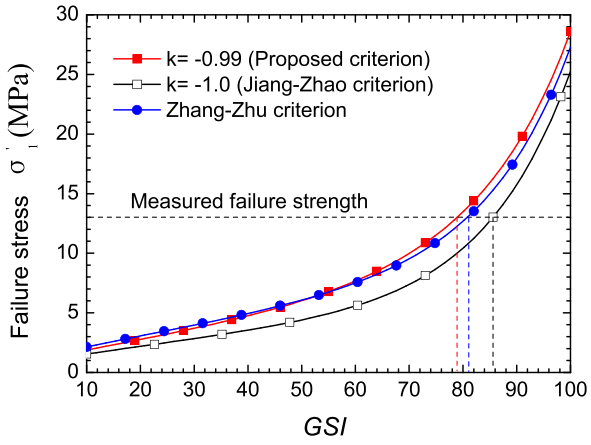

Fig. 12. Variation of failure major principal stress with *GSI* for three failure criteria.

in these literatures. The best-fitting pair m_i and σ_{ci} is identified from TXC data (see Table 2). It is obvious that the model prediction with k=−0.99 fits the test data quite well, whereas that with k=−1 tends to underestimate the strength in both low and high σ'_3 for all rock types. It is worth to be noted that when σ_{ci} is known from the test for Manazuru andesite, Mizuho trachyte and Solnhofen limestone and k=−0.99 is used, only one parameter m_i is required in the new failure criterion. Then the new criterion has the same number of material parameter as the HB criterion, which is extremely easy to use.

5.3. Polyaxial compression of rock masses

PXC test of the rock mass is jointed biotite granite at the Kurobe IV arch dam site in Japan [24], which has been also used to validate other rock failure criteria [4,12]. The test block Q2 was 2.8 m long in the σ'_1 direction, 2.8 m high in the σ'_2 direction and 1.4 m wide in the σ'_3 direction. The unconfined compressive strength of cores of granite was 23.0 MPa and the tested rock mass is undisturbed. The rock mass was described as "somewhat decomposed", and should be more likely in good quality than in very good quality. The measured failure stress σ'_1 of rock masses was 13 MPa by holding σ'_2 and σ'_3 at 0.70 and 0.12 MPa, which is obvious smaller than the cores strength.

Fig. 12 plots the variation of the obtained failure stress σ'_1 with *GSI* (10≤*GSI* ≤100), where D=0 and m_i = 32 was used to calculate parameters m_b, s and a according to Eqs.(8)-(10). The failure stress σ'_1 of the new criterion is obtained according to Eqs. (14) and (15). The result of the Zhang-Zhu criterion [4] is also included in the same figure for comparison purpose. The corresponding *GSI* to the failure strength of 13 MPa for the new criterion (k=−0.99), Jiang-Zhao criterion (k=−1) and Zhang-Zhu criterion is 79, 84 and 81 respectively, which agrees with the description "good surface condition" (70≤*GSI* ≤85) for the test block Q2. Due to the uncertainty of the *GSI* and lacking of more tests data, both TXC and TXE tests on rock masses with detailed characterization are recommended for validating the proposed failure criterion in future.

5.4. Polyaxial compression of cross-anisotropic rock

To formulate the proposed failure criterion for cross-anisotropic rock, the loading direction relative to the microstructure directions of the material is specified using the method proposed by Pietruszczak and Mroz [25,26], which was also used by Lee et al.[8] to study their 3D HB failure criterion. Uniaxial strength σ_{ci} is orientation-dependent, and can be related to the orientation average value σ^0_{ci} by

$$\sigma_{ci} = \sigma^0_{ci}[1 + \Omega_{ij}l_il_j + b_1(\Omega_{ij}l_il_j) + b_2(\Omega_{ij}l_il_j)^3 + b_3(\Omega_{ij}l_il_j)^4 + + b_4(\Omega_{ij}l_il_j)^5 ...] \tag{31}$$

with

$$\Omega_{ij}l_il_j = \Omega_k l_k^2 = \Omega_1 l_1^2 + \Omega_2 l_2^2 + \Omega_3 l_3^2 \tag{32}$$

where $b_i(i = 1, 2, 3...)$ is expansion coefficients, $l_i(i = 1, 2, 3)$ is a unit vector specifying the loading direction relative to the material axes, Ω_{ij} is a tensor describing the deviatoric measurement of the material fabric, and Ω_k is eigenvalues of Ω_{ij}.

$$l_i = \frac{T_i}{\sqrt{\sum_{i=1}^3 L_i^2}} = \frac{\sqrt{\sum_{k=1}^3 \sigma'^2_{jk} e_i^j}}{\sqrt{\sum_{i=1}^3 \left(\sum_{j=1}^3 \sigma'^2_{ij}\right)}} \tag{33}$$

$$\Omega_{ij} = \frac{a_{ij} - \delta_{ij}a_{kk}/3}{a_{kk}/3} \tag{34}$$

where L_i is a resultant stress acting on each plane (see Fig. 13a), T_i is the traction on the plane normal to the principal triad e_i^m; $a_{ij} = a_m e_i^m e_j^m$ is the fabric tensor, and a_m is principal value of the fabric tensor. Seeing from Eq. (31) and (32), the value of σ_{ci} for anisotropic rocks depends on both the stress and fabric tensors.

For cross-anisotropic rocks, the mechanical properties are the same in all directions within the bedding plane. Then $\Omega_2 = \Omega_3$ is obtained, by combining with $\Omega_1 + \Omega_2 + \Omega_3 = 0$, $l_1^2 + l_2^2 + l_3^2 = 1$, Eq. (31) can be simplified to

$$\sigma_{ci} = \sigma^0_{ci}[1 + \Omega_1(1 - 3l_2^2) + b_1\Omega_1^2(1 - 3l_2^2)^2 + b_2\Omega_1^3(1 - 3l_2^2)^3 + b_3\Omega_1^4(1 - 3l_2^2)^4 + b_4\Omega_1^5(1 - 3l_2^2)^5 + ...] \tag{35}$$

where l_2^2 in the principal orientation of the fabric tensor becomes

$$l_2^2 = \frac{\sigma'^2_1\cos^2\alpha + \sigma'^2_2\sin^2\alpha\cos^2\beta + \sigma'^2_3\sin^2\alpha\sin^2\beta}{\sigma'^2_1 + \sigma'^2_2 + \sigma'^2_3} \tag{36}$$

where α is the inclination of the major principal stress to the normal of

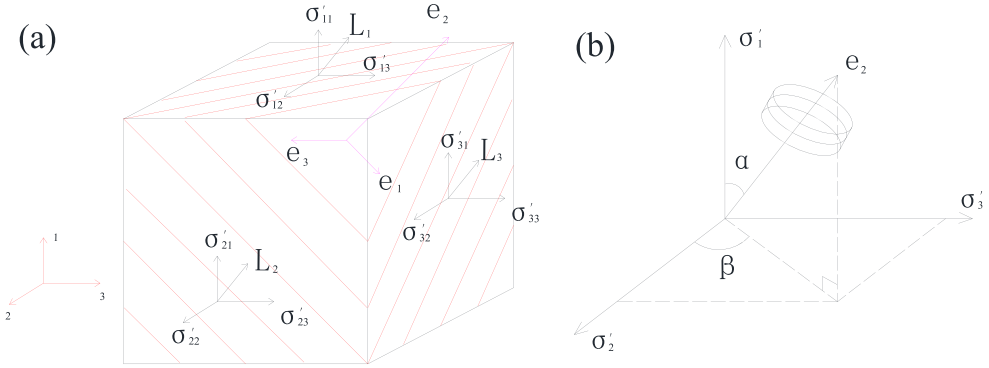

Fig. 13. The loading direction and the principal orientation of the fabric tensor on cross-anisotropic rock: (a) the loading direction, and (b) a projection of the principal orientation of the fabric tensor in 3D stress space.

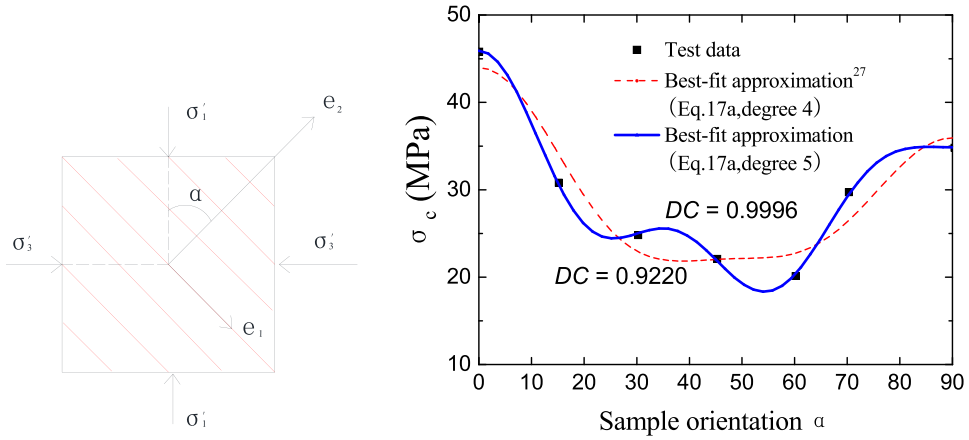

Fig. 14. Variation of uniaxial compressive strength with sample orientation.

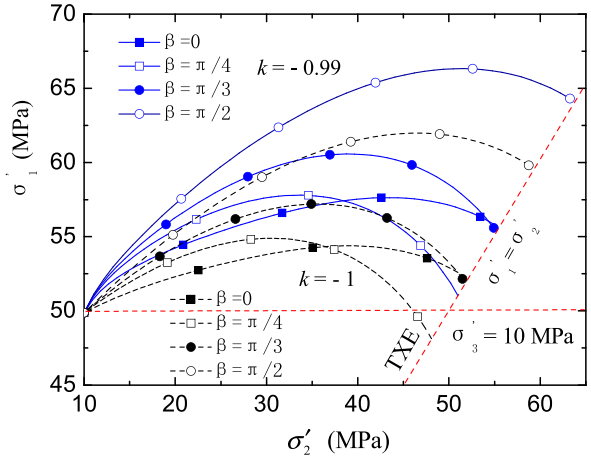

Fig. 15. The influence of the intermediate principal stress on the failure stress for cross-anisotropic rock with four different orientations.

the bedding plane shown in Fig. 13b, and β is the inclination of the intermediate principal stress to the projection of the normal of the bedding plane on the $\sigma_2' - \sigma_3'$ plane. For TXC case ($\sigma_2' = \sigma_3' < \sigma_1'$), Eq. (36) can be written as

$$l_2^2 = \frac{\sigma_1'^2\cos^2\alpha + \sigma_3'^2\sin^2\alpha}{\sigma_1'^2 + 2\sigma_3'^2} \tag{37}$$

Which means that l_2^2 is independent of β.

For a simple loading process ($\sigma_2' = \sigma_3' = 0 < \sigma_1'$), $l_2^2 = \cos^2\alpha$ is obtained from Eq. (37). Then the cross-anisotropic rock in 3D space is reduced to a 2D case. A reasonable approximation of the experimental spatial variation of σ_{ci} is obtained from the best-fitting curves shown in Fig. 14, and the corresponding parameters for two approximation curves are as following:

$$\sigma_{ci}^0 = 22\text{MPa},\ \Omega_1 = 0.0170251,\ b_1 = 515.49,\ b_2 = 61735.3,$$
$$b_3 = 2139820.0 \tag{38}$$

$$\sigma_{ci}^0 = 18.35\text{MPa},\ \Omega_1 = 0.06368,\ b_1 = 328.88,\ b_2 = 2151.50,$$
$$b_3 = -41742.86,\ b_4 = -349803.03 \tag{39}$$

It is evident that the five degree approximation here is better than the four degree approximation given by Pietruszczak et.al.[27] In the following section, the best-fitting parameters in Eq. (39) is used to calculate σ_{ci} in PXC state.

Fig. 15 shows the influence of σ_2' on rock failure for four different orientations $\beta(\beta = 0, \pi/4, \pi/3, \pi/2)$ predicted by the proposed failure criterion, where the minimum principal stress $\sigma_3 = 10$MPa and $\alpha = \pi/3$ are used for demonstration purpose, and m_b=6, s=1,a=0.5 is considered for shale.[8] The results obtained from k=−0.99 are shown in solid lines, whereas the results obtained from k=−1 are indicated by dash lines. It is evident that the orientation angle has a significant influence on the failure stress of the cross-anisotropic rock, and the failure stress corresponding to $\beta = \pi/2$ has the largest value for both k=−0.99 and k=−1, where σ_2' is parallel to the bedding plane. The failure strength in TXC is the same (49.87 MPa) for all orientations because σ_{ci} is independent of β, which can be seen from Eqs. (35) and (37). The failure strength in TXC is lower than the failure strength in TXE except for the case of $\beta = \pi/4$ and k=−1. Based on above findings, it may be concluded that material microstructure (or fabric) can have a significant influence on the failure strength of cross-anisotropic rock in PXC.

6. Conclusions

A new failure criterion with non-circular cross sections is proposed for rocks and concrete based on a unified expression of the 3D HB criteria, which can account for the strength difference between TXE and TXC.

The new criterion includes a shape factor k ($-1 \le k \le 0$) to consider the strength difference in TXC and TXE. It reduces to a lower bound (the Jiang-Zhao 3D HB criterion) with a curved triangle locus in the deviatoric plane when k=−1, and reduces to an upper bound (the Priest 3D HB criterion) with a circle locus in the deviatoric plane when k=0. The failure surface is convex and smooth everywhere when $k \neq -1$, which is very important for plastic flow calculation.

There are three parameters m_i, σ_{ci} and k involved in the new failure criterion for intact rocks and concrete, where m_i and σ_{ci} can be identified using the best fitting method from TXC, and k can be obtained from TXE with fixed m_i and σ_{ci} obtained from TXC. In biaxial plane-stress state, k can be obtained using f_t' and f_{cc}' or σ_{ci}.

Conventional TXC and PXC tests of rocks and concrete, as well as the biaxial compression tests of concrete show that the new failure criterion fits excellently well with the given data, and k=−0.99 is recommended for predicting the rock failure in PXC in the absence of TXE data. Then the proposed failure criterion has the same number of the material parameter as the classical HB criterion.

The proposed failure criterion also performs well for the jointed rock masses in PXC. Finally, the extension of the new failure criterion to PXC of cross-anisotropic rock is discussed. It is found that material microstructure can have a significant influence on the failure strength in PXC.

Acknowledgements

The author thanks to the financial support from the National Science Foundation of China (Grant 51308054),and Fund of National

Engineering and Research Center for Highways in Mountain Area (Grant gsgzj-2012-06), and is grateful to the anonymous reviewers for their helpful comments and suggestions.

References

1 Hoek E, Brown ET. Empirical strength criterion for rock masses. *J Geotech Eng ASCE*. 1980;106(GT9):013–1035.
2 Pan XD, Hudson JA. A simplified three dimensional Hoek–Brown yield criterion. In: Romana M (ed) *Rock Mechanics and Power Plants*. Balkema, Rotterdam; 1998: 95–103.
3 Priest SD. Determination of shear strength and three-dimensional yield strength for the Hoek–Brown criterion. *Rock Mech Rock Eng*. 2005;38(6):299–327.
4 Zhang L, Zhu H. Three-dimensional Hoek–Brown strength criterion for rocks. *J Geotech Geoenviron Eng*. 2007;133(9):1128–1135.
5 Benz T, Schwab R, Kauther RA, Vermeer PA. A Hoek–Brown criterion with intrinsic material strength factorization. *Int J Rock Mech Min Sci*. 2008;45:210–222.
6 Melkoumian N, Priest S, Hunt SP. Further development of the three-dimensional Hoek–Brown yield criterion. *Rock Mech Rock Eng*. 2009;42(6):835–847.
7 Jiang H, Wang XW, Xie YL. New strength criteria for rocks under polyaxial compression. *Can Geotech J*. 2011;48(8):1233–1245.
8 Lee YK, Pietruszczak S, Choi BH. Failure criteria for rocks based on smooth approximations to Mohr–Coulomb and Hoek–Brown failure functions. *Int J Rock Mech Min Sci*. 2012;56:146–160.
9 Jiang H, Zhao JD. A simple three-dimensional failure criterion for rocks based on the Hoek–Brown criterion. *Rock Mech Rock Eng*. 2015;48(5):1807–1819.
10 Jiang H. Three-dimensional failure criteria for rocks based on the Hoek-brown criterion and a general Lode dependence. *Int J Geomech*. 2017;17(8) 04017023-1-12.
11 Willam KJ, Warnke EP. Constitutive model for the triaxial behavior of concrete. Presented at the Seminar on Concrete Structures Subjected to Triaxial Stress. Bergamo, Italy: Istituto Sperimentale Modellie Strutture (ISMES); 1975: 1–30.
12 Zhang Q, Zhu H, Zhang L. Modification of a generalized three-dimensional Hoek–Brown strength criterion. *Int J Rock Mech Min Sci*. 2013;59:80–96.
13 Priest SD. Three-dimensional failure criteria based on the Hoek–Brown criterion. *Rock Mech Rock Eng*. 2012;45(6):989–993.
14 Murrell SAF. A criterion for brittle fracture of rocks and concrete under triaxial stress, and the effect of pore pressure on the criterion. In: Fairhurst C (ed) *Proceedings of the 5th Symposium on Rock Mechanics*. Minneapolis: University of Minnesota; 1963: 563–577.
15 Handin J, Heard HC, Magouirk JN. Effect of the intermediate principal stress on the failure of limestone, dolomite, and glass at different temperature and strain rate. *J Geophys Res*. 1967;72:611–640.
16 Mogi K. Experimental Rock Mechanics, London: Taylor & Francis; 2007.
17 Phueakphum D, Fuenkajorn K, Walsri C. Effects of intermediate principal stress on tensile strength of rocks. *Int J Fract*. 2013;181(2):163–175.
18 Mills LL, Zimmerman RM. Compressive strength of plain concrete under multiaxial loading conditions. *Acids J Proc*. 1970:802–807.
19 Launay P, Gachon H. Strain and ultimate strength of concrete under triaxial stresses. *Acids Spec Pub*. 1972;1:269–282.
20 Kupfer H, Hilsdorf HK, Rusch H. Behavior of concrete under biaxial stresses. *Acids J*. 1969;66(8):545–666.
21 Tasuji ME, Slate FO, Nilson AH. Stress-strain response and fracture of concrete in biaxial loading. *Acids J*. 1978;75(7):306–312.
22 Eberhardt E. The Hoek–Brown failure criterion. *Rock Mech Rock Eng*. 2012;45:981–988.
23 Colmenares LB, Zoback MD. A statistical evaluation of intact rock failure criteria constrained by polyaxial test data for five different rocks. *Int J Rock Mech Min Sci*. 2002;39(6):695–729.
24 Müller-Salzburg L, Ge X. Untersuchungen Zum Mechanischen Verhallen Gekl ¨ ufteten Gebirges unter Wechsellasten. In: *Proceedings of the 5th Congress International Society Of Rock Mechanics*. Rotterdam; 1983: 43–49.
25 Pietruszczak S, Mroz Z. Formulation of anisotropic failure criteria incorporating a microstructure tensor. *Comput Geotech*. 2000;26:105–112.
26 Pietruszczak S, Mroz Z. On failure criteria for anisotropic cohesive-frictional materials. *Int J Numer Anal Methods Geomech*. 2001;25(5):509–524.
27 Pietruszczak S, Lydzba D, Shao JF. Modelling of inherent anisotropy in sedimentary rocks. *Int J Solids Struct*. 2002;39:637–648.